The Plant Cell, Vol. 17, 1625–1636, May 2005, www.plantcell.org

The Sulfate Transporter SST1 Is Crucial for Symbiotic Nitrogen Fixation in *Lotus japonicus* Root Nodules

Lene Krusell,[a] Katja Krause,[a] Thomas Ott,[a] Guilhem Desbrosses,[a] Ute Krämer,[a] Shusei Sato,[b] Yasukazu Nakamura,[b] Satoshi Tabata,[b] Euan K. James,[c] Niels Sandal,[d] Jens Stougaard,[d] Masayoshi Kawaguchi,[e] Ai Miyamoto,[f] Norio Suganuma,[f] and Michael K. Udvardi[a,1]

[a] Max Planck Institute of Molecular Plant Physiology, 14476 Golm, Germany
[b] Kazusa DNA Research Institute, Kisarazu, Chiba 292-0812, Japan
[c] School of Life Sciences, University of Dundee, Dundee DD1 5EH, United Kingdom
[d] Department of Molecular Biology, University of Aarhus, DK-8000 Aarhus, Denmark
[e] Department of Biological Sciences, University of Tokyo, Hongo, Tokyo 113-0033, Japan
[f] Department of Life Science, Aichi University of Education, Kariya, Aichi 448-8542, Japan

Symbiotic nitrogen fixation (SNF) by intracellular rhizobia within legume root nodules requires the exchange of nutrients between host plant cells and their resident bacteria. Little is known at the molecular level about plant transporters that mediate such exchanges. Several mutants of the model legume *Lotus japonicus* have been identified that develop nodules with metabolic defects that cannot fix nitrogen efficiently and exhibit retarded growth under symbiotic conditions. Map-based cloning of defective genes in two such mutants, *sst1-1* and *sst1-2* (for symbiotic sulfate transporter), revealed two alleles of the same gene. The gene is expressed in a nodule-specific manner and encodes a protein homologous with eukaryotic sulfate transporters. Full-length cDNA of the gene complemented a yeast mutant defective in sulfate transport. Hence, the gene was named *Sst1*. The *sst1-1* and *sst1-2* mutants exhibited normal growth and development under nonsymbiotic growth conditions, a result consistent with the nodule-specific expression of *Sst1*. Data from a previous proteomic study indicate that SST1 is located on the symbiosome membrane in Lotus nodules. Together, these results suggest that SST1 transports sulfate from the plant cell cytoplasm to the intracellular rhizobia, where the nutrient is essential for protein and cofactor synthesis, including nitrogenase biosynthesis. This work shows the importance of plant sulfate transport in SNF and the specialization of a eukaryotic transporter gene for this purpose.

INTRODUCTION

Nitrogen-fixing symbioses between legume plants and soil bacteria called rhizobia are among the most important symbioses on earth: they are not only a major source of fixed nitrogen for natural ecosystems but also the single largest natural source of nitrogen for agriculture (Smil, 1999). Symbiotic nitrogen fixation (SNF) in legumes takes place in specialized organs called nodules that develop from dedifferentiated root cells after infection by specific rhizobia in the soil. Rhizobia colonize developing nodule tissue via infection threads (Brewin, 1991) and ultimately enter cortical cells by endocytosis (Verma and Hong, 1996). This results in a novel organelle called the symbiosome that consists of one or more bacteria surrounded by the plant peribacteroid or symbiosome membrane (SM) (Roth and Stacey, 1989). Structurally similar organelles exist in many intracellular symbioses, including important parasitic symbioses of humans such as malaria, Leishmania, and Legionnaire's disease (Roth et al., 1988). Rhizobia that enter cortical cells continue to multiply until cells of the developing nodule are literally packed with thousands of bacteria, enclosed individually or in small groups within symbiosomes. Nodule development is accompanied by coordinated differentiation of both plant and bacterial cells, which involves global changes in gene expression in both partners (Colebatch et al., 2002, 2004; Fedorova et al., 2002; Ampe et al., 2003; Becker et al., 2004; Kouchi et al., 2004; Kuster et al., 2004; Uchiumi et al., 2004). Many of these changes affect plant and bacterial metabolism and transport, which ultimately become specialized to support the exchange of reduced carbon and other nutrients from the plant for reduced nitrogen from the bacteroids (Lodwig et al., 2003). The SM plays a key role in controlling such exchanges (Udvardi and Day, 1997).

At the heart of legume–rhizobia symbiosis is the bacterial metalloenzyme nitrogenase, which is composed of two proteins, called the Fe protein and the MoFe protein. The metalloclusters contained within nitrogenase include a typical [4Fe-4S] cluster bridged between identical subunits of the Fe protein and two novel clusters contained within the MoFe protein, designated the P cluster and FeMo cofactor (Dos Santos et al., 2004).

[1] To whom correspondence should be addressed. E-mail udvardi@mpimp-golm.mpg.de; fax 49-331-567-8250.
The authors responsible for distribution of materials integral to the findings presented in this article in accordance with the policy described in the Instructions for Authors (www.plantcell.org) are: Jens Stougaard (stougaard@mb.au.dk), Norio Suganuma (nsuganum@auecc.aichi-edu.ac.jp), and Michael Udvardi (udvardi@mpimp-golm.mpg.de).
Article, publication date, and citation information can be found at www.plantcell.org/cgi/doi/10.1105/tpc.104.030106.

Biochemical, biophysical, and cell biological studies have revealed the presence of a variety of transporters on the SM of different legume species: P-type H^+-ATPases (Bassarab et al., 1986; Domigan et al., 1988; Udvardi and Day, 1989; Andreev et al., 1997; Rojas-Ojeda et al., 1998; Fedorova et al., 1999); a dicarboxylate transporter (Udvardi et al., 1988); ammonium and ammonia channels (Tyerman et al., 1995; Niemietz and Tyerman, 2000); iron transporters (Moreau et al., 1995; LeVier et al., 1996; Moreau et al., 1998); calcium pumps and channels (Andreev et al., 1999; Roberts and Tyerman, 2002); aquaporins/ion channels (Fortin et al., 1987; Miao et al., 1992; Weaver et al., 1994; Rivers et al., 1997; Dean et al., 1999); and cation and anion channels/transporters (Udvardi et al., 1991; Roberts and Tyerman, 2002). Few genes encoding SM transporters have been identified to date; these include the aquaporin nodulin 26 (Fortin et al., 1987), a zinc transporter (Moreau et al., 2002), and an iron transporter (Kaiser et al., 2003). Transcriptome analyses have revealed a plethora of nodule-induced transporter genes, some of which may encode SM proteins (Colebatch et al., 2002; Fedorova et al., 2002). Proteomic studies of isolated SM from various legume species identified numerous proteins associated with this membrane, including several transporters (Panter et al., 2000; Saalbach et al., 2002; Wienkoop and Saalbach, 2003; Catalano et al., 2004).

Genetics has played a decisive role in identifying bacterial and plant genes that are crucial to SNF. Transposon insertion and deletion mutagenesis in rhizobia led to the identification of many bacterial genes that are essential for SNF, including multiple *nif* (for nitrogen fixation), *nod* (for nodulation), and *fix* (for symbiotic fixation) genes (Long, 2001). The development of genetic resources for model legumes with relatively small diploid genomes, especially *Lotus japonicus* and *Medicago truncatula*, has facilitated the recent discovery of a smaller number of plant genes involved in nodule development (Schauser et al., 1999; Endre et al., 2002; Krusell et al., 2002; Nishimura et al., 2002a, 2002b; Stracke et al., 2002; Limpens et al., 2003; Madsen et al., 2003; Radutoiu et al., 2003; Searle et al., 2003; Ana et al., 2004; Levy et al., 2004; Mitra et al., 2004). However, relatively little attention has been given to genes that are required for plant cell differentiation during nodule development, especially those required for metabolic differentiation. One exception is a gene that encodes nodule-induced sucrose synthase, which has been shown to be important for carbon and energy metabolism in pea nodules and for SNF (Gordon et al., 1999). Two other examples, from reverse rather than forward genetics, are glutamate synthase and leghemoglobin, which are required for nitrogen assimilation and oxygen transport/energy metabolism in nodules, respectively (Cordoba et al., 2003; Ott et al., 2005). To identify other plant genes with central roles in nodule metabolism and SNF, we have undertaken map-based cloning of Lotus *sym* (for symbiosis) genes that are required for nodule function but not nodule development per se. Here, we describe the identification of a gene, *Sst1* (for symbiotic sulfate transporter), that encodes a nodule-specific sulfate transporter that is essential for SNF in Lotus. This plant transporter has an indispensable role in a mutualistic symbiosis. It also demonstrates a successful map-based cloning of a gene with a crucial role in legume nodule function.

RESULTS

The *sst1-1* and *sst1-2* Mutant Phenotypes

Several Lotus *sym* mutants that develop nonfunctional nodules have been identified via independent mutagenesis projects (Schauser et al., 1998; Kawaguchi et al., 2002). The *sst1-1* and *sst1-2* monogenic recessive mutants (formerly named *sym13* and *sym81*, respectively; see Methods) display nitrogen deficiency symptoms under symbiotic conditions: yellow leaves, anthocyanin production in the stem, strong reduction of shoot growth, and a concomitant increase in root:shoot ratio (Figure 1A). On the other hand, the mutants exhibit a wild-type phenotype with respect to growth and development under nonsymbiotic growth conditions. Crosses between *sst1-1* and *sst1-2* did not result in genetic complementation of the symbiotic defect, which indicated an allelic relationship between the two. This was confirmed by map-based cloning (see below). Both mutants develop nodules that are smaller than mature wild-type nodules (Figures 1B to 1D) and that senesce prematurely. Mutant nodules are typically pink before senescence, and immunogold labeling confirmed the presence of leghemoglobin in the cytoplasm of infected cells of *sst1-1* nodules (Figure 2H). However, gold particle counts indicated a 30% reduction in leghemoglobin in mutant versus wild-type nodules, which may reflect the failure of SNF and early senescence in mutant nodules (mean counts $\pm$ SE in cytoplasm of 10 micrographs taken at $\times$30,000 [i.e., an area of 11 μm^2] were 24.0 $\pm$ 2.3 for wild-type nodules and 16.3 $\pm$ 1.3 for *sst1-1* mutant nodules). Immunogold labeling using an antibody raised against the NifH subunit of nitrogenase showed a similar reduction in the amount of this protein in bacteroids of mutant versus wild-type nodules (Figure 2): gold particle counts

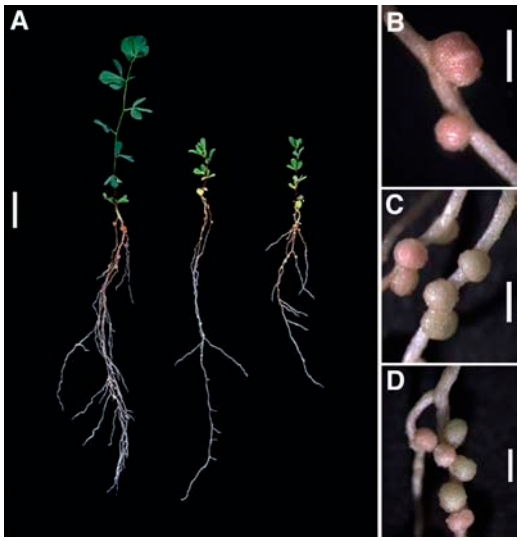

Figure 1. Symbiotic Phenotypes of *sst1-1* and *sst1-2*.

Plants were inoculated with *M. loti* and grown in quartz sand without mineral nitrogen for 4 weeks in a greenhouse, as described in Methods.
(A) Wild type, left; *sst1-1*, middle; *sst1-2*, right. Bar = 2 cm.
(B) to **(D)** Close-up views of nodules from the wild type **(B)**, *sst1-1* **(C)**, and *sst1-2* **(D)**. Bars = 1 mm.

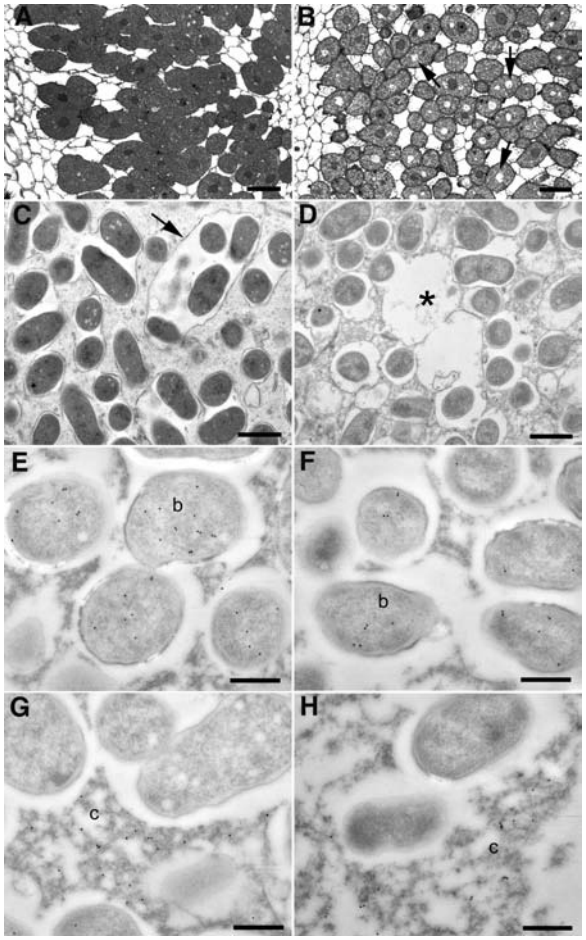

Figure 2. Comparison of Wild-Type and *sst1* Mutant Nodule Ultrastructure at 21 d after Inoculation.

Plants were inoculated with *M. loti* and grown in clay beads without mineral nitrogen in a greenhouse, as described in Methods.
(A) Light micrograph of a mature wild-type nodule showing infected cells packed with bacteria.
(B) Light micrograph of an *sst1-1* mutant nodule showing infected cells containing several vacuoles (arrows), which may be associated with lysis of the bacteroids.
(C) Transmission electron micrograph of an infected cell of a mature wild-type nodule containing bacteroids within intact symbiosomes surrounded by SM (arrow).
(D) Transmission electron micrograph of an infected cell of a mature *sst1-1* mutant nodule showing the formation of a lytic vacuole (asterisk).
(E) Transmission electron micrograph showing strong immunogold labeling of NifH protein inside bacteroids (b) of a wild-type nodule.
(F) Transmission electron micrograph showing weak immunogold labeling of NifH protein inside bacteroids (b) of an *sst1-1* mutant nodule.
(G) Transmission electron micrograph showing immunogold labeling of leghemoglobin in the cell cytoplasm (c) of a wild-type nodule.
(H) Immunogold labeling of leghemoglobin in the cell cytoplasm (c) of an *sst1-1* mutant nodule showing slightly reduced levels of the protein.
Bars = 50 μm in **(A)** and **(B)**, 1 μm in **(C)** and **(D)**, and 500 nm in **(E)** to **(H)**.

were 9.1 ± 0.8 for wild-type nodules and 6.2 ± 0.9 for *sst1-1* mutant nodules (mean counts ± SE of 32 bacteroids in 10 micrographs taken at ×30,000).

Detailed analysis of the growth, nodulation, and nitrogen fixation of the *sst1-2* mutant over a 12-week period revealed that the rate of nitrogen fixation, measured as acetylene reduction activity, was reduced by ~90% in *sst1-2* plants compared with wild-type plants, which accounted for the substantially slower growth of the mutant (Figure 3). Nitrogen deficiency probably also explains the increased numbers of

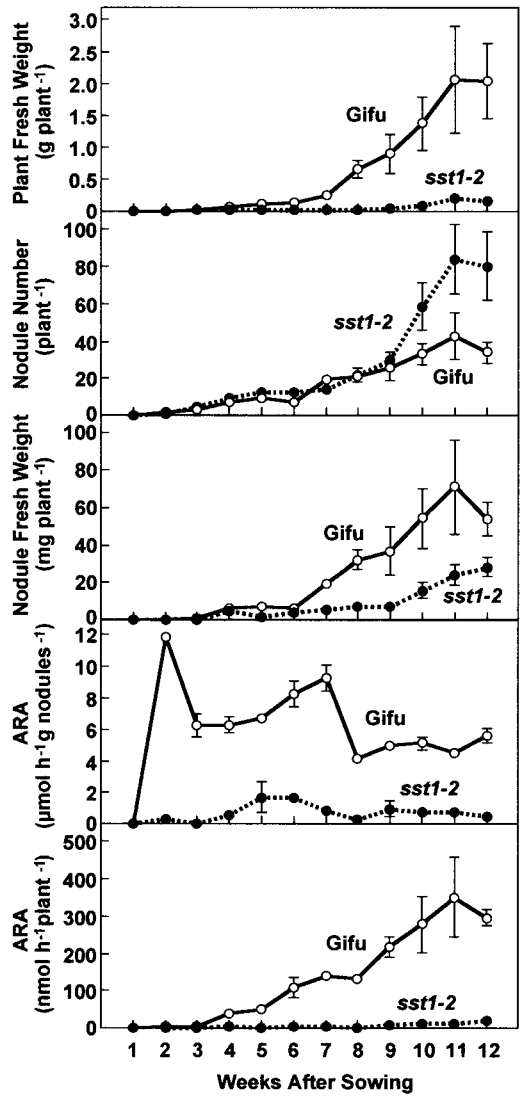

Figure 3. Growth, Nodulation, and Nitrogen Fixation Phenotypes of *sst1-2*.

Plants were inoculated with *M. loti* and grown in quartz sand without mineral nitrogen in a greenhouse, as described in Methods. Plant fresh weight, number of nodules, nodule fresh weight, and acetylene reduction activity (ARA) in the wild-type Gifu and the *sst1-2* mutant during plant development are shown. All values are means of three determinations, and the vertical bars indicate SE.

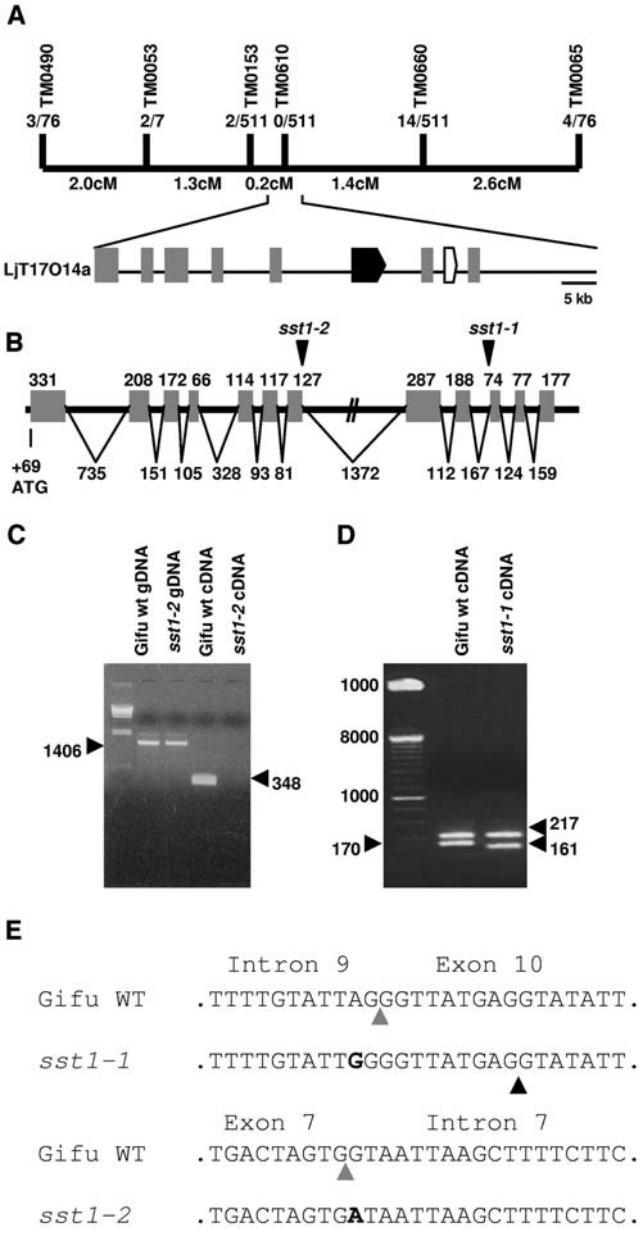

Figure 4. Map-Based Cloning of *Sst1* and Molecular Analysis of the Mutations.

(A) Genetic map of the *Sst1* region with markers and numbers of recombinants indicated above the line. Genetic distance in centimorgan (cM) is indicated below the line. The physical map of the sequenced TAC clone LjT17O14a is shown. The *Sst1* gene is indicated as a black arrow, and a duplicated region containing exon 8 to exon 12 of *Sst1* is indicated as a white arrow. Retrotransposon-related sequences are indicated as gray boxes.

(B) Intron–exon structure of the *Sst1* gene with sizes (bp) of exons and introns indicated above and below the line, respectively. Black arrowheads mark the positions of mutations in the *sst1-1* and *sst1-2* alleles.

(C) PCR analysis of *Sst1* genomic DNA (lanes 2 and 3) and cDNA (lanes 4 and 5) from wild-type plants (lanes 2 and 4) and *sst1-2* plants (lanes 3 and 5) using primers flanking the *sst1-2* mutation site. Note the absence of a PCR amplicon from cDNA of the mutant (lane 5).

nodules on mutant plants later in plant development (Figures 1 and 3), as nodule development is feedback-inhibited by fixed nitrogen (Wopereis et al., 2000).

Map-Based Cloning of the *Sst1* Gene

A positional cloning strategy was used to identify the gene affected in the *sst1-1* and *sst1-2* mutants. A combined mapping population of 511 F2 mutant plants was generated by crossing *sst1-1* and *sst1-2* with the wild-type Lotus ecotype MG20. The mutant loci were initially positioned on the upper arm of chromosome II on the genetic map of Lotus using microsatellite markers (Sandal et al., 2002). Fine mapping localized the mutations to a region of 1.6 centimorgan between markers TM0153 and TM0660, which spanned TM0610, a marker that exhibited no recombination events in the 511 plants analyzed (Figure 4). A draft sequence of the transformation-competent artificial chromosome (TAC) clone containing TM0610 was obtained and potential open reading frames and seven retrotransposon-related sequences were identified by comparison with sequences in the National Center for Biotechnology Information (NCBI) database (http://www.ncbi.nlm.nih.gov/). A single gene known to be expressed in Lotus was found on TM0610; it encodes a putative sulfate transporter that is induced greatly during nodule development (Colebatch et al., 2002) and corresponds to Lotus tentative consensus sequences (TCs) 8880 and 8045 in The Institute for Genomic Research (TIGR) database (http://www.tigr.org/tigr-scripts/tgi/T_index.cgi?species=l_japonicus). The encoded protein had been located on the SM of Lotus (Wienkoop and Saalbach, 2003), a strategic position for controlling plant–bacteroid nutrient interactions. Thus, this gene/protein became the prime suspect for further work.

The gene encoding the putative sulfate transporter, which we named *Sst1*, was cloned from both *sst1-1* and *sst1-2* and sequenced. A single nucleotide substitution changing the AG/GG splice site of intron 9/exon 10 to GGGG was identified in the *sst1-1* allele. PCR amplification and sequencing of a fragment covering the mutation site using *sst1-1* cDNA as template showed that intron 9 is spliced using an alternative splice site nine nucleotides into exon 10 (Figure 4), which results in the loss of three amino acids in the SST1-1 mutant protein (537-RVM-539) (Figure 5). The Arg in this sequence is highly conserved among plant sulfate transporters. A single nucleotide substitution at the exon 7/intron 7 splice site (TG/GT→TGAT) of the *sst1-2* allele was identified, which presumably results in an

(D) PCR performed on cDNA from the wild type (lane 2) and *sst1-1* (lane 3) using primers flanking the *sst1-1* mutation site. PCR amplicons were digested with *Bgl*II before gel electrophoresis, which resulted in two fragments of 217 and 170 bp in the wild type. Note the downshift in the smaller of these bands from *sst1-1*, corresponding to a loss of nine nucleotides in the mutant transcript.

(E) Indication of the mutations in the *sst1-1* and *sst1-2* alleles. Light gray arrowheads indicate the splice sites in the wild type (WT), whereas the black arrowhead indicates the position of the alternative splice site of the *sst1-1* mutant allele. The nucleotide changes in the two mutant alleles are indicated in boldface.

MGTIGNNSHEGDHHGVNFTAQRGFYTKLKSGLKETFFPDD
PFRQIKEEENRSRRIIKGVQYYVPIFEWLPNYTLRLFISD
FISGLTITSLAIPQGISYAKLANLPPIVGLYSSFVPPLVY
AIFGSSRHMAVGTLAAASLLIGQTISTVASPETDPTLYLH
LIFTTTFVTGVFQACLGIFRLGILVDFFSHSTITGFMGGT
AFILIAQQLKGFFGMKHFSTKTNLVEVAKSIITNRHEIRW
ETTVLGLVFLAFLQFTRHVRNKRPKLFWVSAIAPMTVVIV
GSIFVYLVHGQKHGIPIVGHLDRGLNPWSIQYFNFDSKYL
PAVMQAALITGVLSLAEGIAIGRSFSVTDNTPHDGNKEMV
AFGLMNLFGSFTSCYLTSGPFSKTAVNYNAGGKTAMTNVV
QAVLMALTLQFLAPLFGFTPLVALSAIITSAMLGLVNYTE
VIYLYKVDKFDFVICMAAFLGVAFLGMDYGLMISVGLGVI
RALLYVARPATCKLGKLNEFGIYRDVEQYPASTFPGLIIV
QLGSPVYFSNSVYVKERVMRYIKSQQRSNEDVVEQVILDM
SGVTSIDTTAIEGLLELNKMLEKNGIEMFLVNPRLEVMEK
LIISKFVDKLGKESFYLTLDDAVKASQYSLKKNDNGDIVH
ETSHA

Figure 5. Features of the SST1 Amino Acid Sequence.

Putative transmembrane domains are underlined. The three amino acids, RVM, deleted in the *sst1-1*mutant protein are indicated in boldface. Conserved residues of the STAS domain are highlighted in light gray.

inability to splice intron 7. *Sst1* mRNA was not detectable in nodules of *sst1-2* by RT-PCR, indicating that the mutant transcript is unstable (Figure 4). Intron 7 contains a stop codon, which would terminate translation of the *sst1-2* transcript prematurely. Therefore, the lack of *sst1-2* transcript in the mutant could be explained by nonsense-mediated mRNA decay (Mitra et al., 2004).

A full-length cDNA corresponding to the *Sst1* gene was identified in an EST collection originating from Lotus nodules (Colebatch et al. 2002) and completely sequenced. The 2352-bp cDNA contains an open reading frame of 1938 bp preceded by a 68-bp 5′ leader sequence and a 3′ untranslated region of 346 bp. Comparison of the *Sst1* gene and cDNA sequences revealed 12 exons in the gene (Figure 4). The SST1 protein consists of 645 amino acids with a predicted mass of 71.4 kD (Figure 5). The protein is also predicted to contain 12 membrane-spanning domains, with cytoplasmic N- and C-terminal ends, similar to other plant sulfate transporters (Hawkesford, 2003). The C terminus contains a predicted STAS domain (for sulfate transporter and antisigma-factor antagonists). The STAS domain was identified originally in bacterial antisigma-factor antagonists and is believed to form a tertiary structure involved in nucleotide triphosphate binding and protein–protein interaction. The STAS domain has been identified in anion transporters in eukaryotes and many bacteria (Aravind and Koonin, 2000).

Developmental Regulation of the *Sst1* Gene

Although the *sst1-1* and *sst1-2* mutants do not exhibit any obvious defects in growth or development under nonsymbiotic conditions, we were interested to know whether the *Sst1* gene is expressed in organs other than nodules. Transcripts of *Sst1* were detected in nodules but not in roots, cotyledons, stems, leaves, flowers, or pods of Lotus plants by RNA gel blot analysis. Using the more sensitive technique of real-time RT-PCR, *Sst1* transcripts were detected in roots and leaves, but at levels just 4 and 1%, respectively, of those in nodules (Figure 6). *Sst1* is represented by 53 ESTs in the two Lotus TC contigs, TC8045 and TC8880, in the TIGR database, and 52 of these ESTs are derived from nodules. The single remaining EST comes from a cDNA library of nodulated roots. No EST for *Sst1* comes from noninoculated roots, shoots, or any other organ. Thus, *Sst1* appears to have evolved a symbiosis-specific function. Further analysis of the timing of *Sst1* induction during nodule development revealed that the gene is induced at a relatively late stage, slightly after the archetypal late nodulin, leghemoglobin (Figure 6). Thus, like leghemoglobin, *Sst1* is a late nodulin.

Functional Characterization of the SST1 Protein

Plant sulfate transporter homologs have been sorted into five groups, based on phylogenetic analysis of protein sequences (Hawkesford, 2003). None of the transporters of homologous

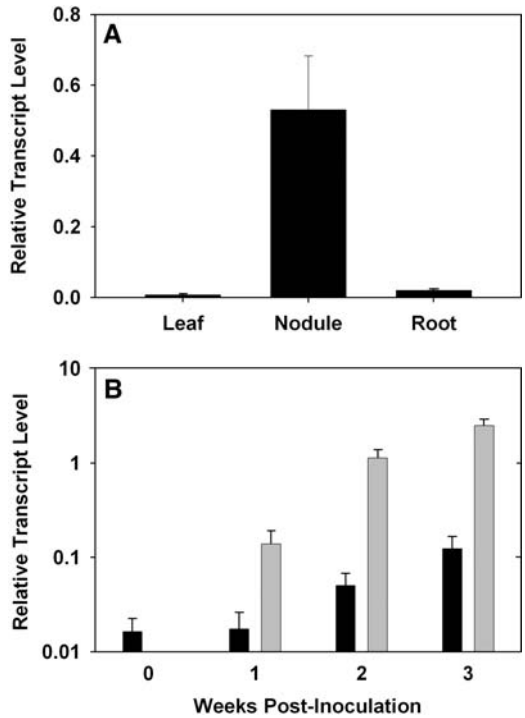

Figure 6. Developmental Regulation of *Sst1* Expression.

Plants were inoculated with *M. loti* and grown under sterile conditions on agar plates, as described in Methods.

(A) Relative transcript level for *Sst1* in different organs.

(B) Time course of *Sst1* expression in inoculated roots, including nodules (black bars). Transcript levels for leghemoglobin (gray bars) are included for comparison. Note the logarithmic scale on the *y* axis. All transcript levels are expressed relative to those of ubiquitin in the same sample.

group 3 putative plant sulfate transporters, which includes SST1 (Figure 7), has been shown to transport sulfate. To demonstrate this for SST1, a full-length *Sst1* cDNA was expressed in yeast mutant strain CP154-7A, which is defective in two high-affinity sulfate transporters and cannot grow on low concentrations of sulfate (Cherest et al., 1997). Expression of *Sst1* in the yeast double mutant rescued growth on minimal medium containing 0.5 mM Mg_2SO_4 as sole sulfur source (Figure 8). Thus, SST1 is the first member of group 3 in plants to be confirmed as a sulfate transporter.

Given that SST1 is able to transport sulfate when expressed in yeast cells, we were interested to know whether nodules of the *sst1-1* and *sst1-2* mutants contained lower concentrations of total sulfur than wild-type nodules. Element analysis by inductively coupled plasma optical emission spectroscopy (ICP-OES) showed that the relative total sulfur concentrations were decreased by 24.1% ± 9.1% (mean ± SD; $n = 3$ independent experiments) in *sst1-1* nodules and by 19.6% ± 6.9% (mean ± SD; $n = 2$ independent experiments) in *sst1-2* nodules compared with wild-type nodules.

DISCUSSION

SNF in legumes takes place in specialized organs called root nodules, which develop from root cells after contact with specific rhizobia in the soil under conditions of nitrogen limitation. Legumes invest a lot in the molecular infrastructure of nodules to win a reliable source of fixed nitrogen from SNF. For instance, the concentration of protein in legume nodules is more than 30 times higher than in the roots, whereas phosphate and fatty acid concentrations are between three and four times higher in nodules than in roots (Gaude et al., 2004). Much of the phosphate of nodule cells is presumably invested in rRNA to support the high rates of protein synthesis and metabolic activity in this organ. Interestingly, more than half of the protein and approximately one-third of the phosphate of nodules are present in the bacteroids (Gaude et al., 2004). Essentially all of the inorganic and organic building blocks for nodule development are imported from other organs. For instance, sugars derived from photosynthesis in the shoot are imported into nodules via the phloem for carbon and energy metabolism (Day and Copeland, 1991), whereas mineral forms of nitrogen, phosphorus, and sulfur together with the many micronutrients required for cellular metabolism are provided principally by the root after acquisition from the soil. Import of nutrients into nodules involves both phloem and xylem, and transfer of nutrients from the vascular tissue to other tissues, cells, and organelles, including symbiosomes containing the bacteroids, must involve numerous transporters within different membranes.

EST projects have revealed hundreds of genes encoding putative transport proteins that are expressed in nodules of different legume species, including Lotus (Colebatch et al., 2002,

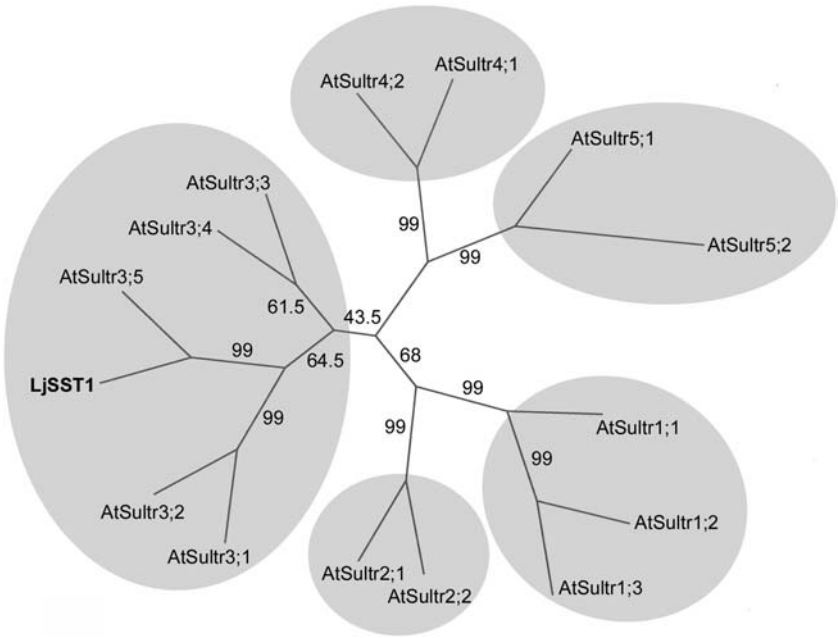

Figure 7. Phylogenetic Analysis of Sulfate Transporters from *Arabidopsis thaliana* and LjSST1 from *Lotus japonicus*.

The nomenclature of Hawkesford (2003) was used: AtSulftr1;1 = At4g08620, AtSulftr1;2 = At1g78000, AtSulftr1;3 = At1g22150, AtSulftr2;1 = At5g10180, AtSulftr2;2 = At1g77990, AtSulftr3;1 = At3g51895, AtSulftr3;2 = At4g02700, AtSulftr3;3 = At1g23090, AtSulftr3;4 = At3g15990, AtSulftr3;5 = At5g19600, AtSulftr4;1 = At5g13550, AtSulftr4;2 = At3g12520, AtSulftr5;1 = At1g80310, and AtSulftr5;2 = At2g25680. Full-length amino acid sequences were aligned using ClustalW (http://clustalw.genome.ad.jp/) and analyzed with the PHYLIP software package (http://www.csc.fi/molbio/progs/phylip/doc/main.html). Bootstrap values were obtained from 100 replicates. The branch lengths indicate the frequency of the corresponding clade in the set of bootstrap trees.

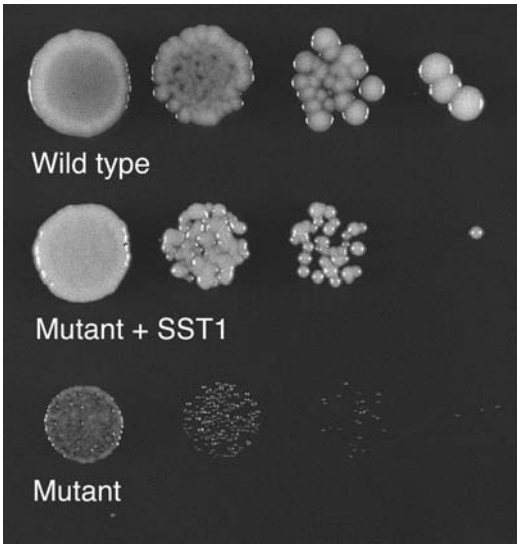

Figure 8. Functional Complementation of Yeast Sulfate Transporter Mutant CP154-7A by SST1.

Yeast strains were grown on minimal medium containing 0.5 mM $MgSO_4$ as sole sulfur source. Cells were spotted in a 10-fold dilution series from left to right. A wild-type strain transformed with the expression vector p112A1NE (top row) was included as a positive control for mutant strain CP154-7A transformed with *Sst1* cDNA in p112A1NE (middle row). The mutant strain containing p112A1NE (bottom row) was included as a negative control.

2004; Fedorova et al., 2002; El Yahyaoui et al., 2004; Kouchi et al., 2004; Kuster et al., 2004). Many of these genes are induced during nodule development, and some are virtually nodule-specific, which indicates that they play highly specialized roles in this organ. Among the latter are genes encoding transporters of the SM, including *Sst1* (Colebatch et al., 2002; Wienkoop and Saalbach, 2003). Other transporter genes that are induced during nodule development include putative sugar transporters, which presumably distribute the products of photosynthesis to cells throughout the nodule, and amino acid transporters, which may play a role in amino acid export from the nodule to the rest of the plant (Flemetakis et al., 2003; Colebatch et al., 2004; El Yahyaoui et al., 2004; Kouchi et al., 2004). Despite the ever-growing list of plant transporter genes known to be expressed in nodules, none has been found to be essential for SNF.

Map-based cloning yielded two mutant alleles, *sst1-1* and *sst1-2*, of a gene that is crucial for SNF in nodules (Figure 4). Sequence analysis indicated that the gene encodes a sulfate transporter, and this was confirmed by functional expression of the wild-type SST1 protein in yeast (Figure 8). Thus, SST1 is the first transporter to be identified that is crucial for SNF. Quantitative RT-PCR showed that expression of *Sst1* is essentially nodule-specific (Figure 6), which suggests that the *Sst1* gene evolved to fulfill a symbiosis-specific function. Consistent with this idea is the fact that mutations in the gene had no obvious effect on plant growth and development under nonsymbiotic conditions.

What is the precise role of SST1 in nodules? Proteomic data indicate that SST1 is located on the SM of Lotus nodules (Wienkoop and Saalbach, 2003), which suggests that SST1 may be responsible for transporting sulfate from the host cell cytoplasm to the bacteroids. As the SM is unique to nodules, the location of SST1 in this membrane is consistent with both nodule-specific expression of the *Sst1* gene and the symbiosis-specific phenotype of *sst1* mutants. Sulfur is an important component of many biological molecules, including proteins and protein co-factors. As mentioned above, bacteroids contain approximately half of the total protein in legume nodules (Gaude et al., 2004). The nitrogenase structural proteins NifH, NifD, and NifK are among the most abundant proteins in bacteroids. Each active nitrogenase complex consists of two NifH, a NifD, and a NifK subunit, with a total of 75 S-containing amino acids in the *Mesorhizobium loti* complex, and four metal-sulfur clusters ([4Fe-4S], [8Fe-7S], [4Fe-3S], and [3Fe-Mo-3S]), which provide a conduit for electron flow to N_2 (Dos Santos et al., 2004). A model illustrating the possible role of SST1 in nodules is presented in Figure 9. Disruption of sulfate transport into symbiosomes could account for the lower level of NifH protein observed in *sst1-1* mutant nodules compared with the wild type. It would also affect a major sink for S in nodules, which conceivably could lead to a reduction in the total amount of S that accumulates in nodules. In fact, this is what was found for nodules of the *sst1-1* and *sst1-2* mutants using ICP-OES.

Various auxotrophs of rhizobia have been used to gain insight into the types of nutrients that are provided by legumes to nitrogen-fixing bacteroids in nodules. For instance, a Met auxotroph of *Rhizobium leguminosarum* formed effective nitrogen-fixing nodules on the roots of pea (Pain, 1979), suggesting that bacteroids receive ample Met from host cells in pea nodules. By contrast, mutants of *R. meliloti* defective in Met biosynthesis

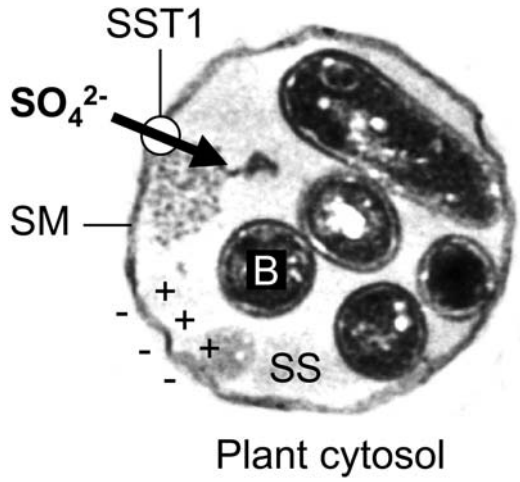

Figure 9. Proposed Role of SST1 in Nodule Symbiosome Sulfate Transport.

Based on data presented here and elsewhere (Wienkoop and Saalbach, 2003), SST1 is proposed to transport sulfate across the SM from the plant cell cytoplasm into the symbiosome space (SS), where it is available to nitrogen fixing bacteroids (B). Anion transport into symbiosomes is favored by the net positive charge on the inside surface of the SM, which is generated by an H^+-ATPase (data not shown).

formed nodules on alfalfa that were unable to fix nitrogen, indicating that Met supply from the host in this case was insufficient to meet bacteroid needs (Kerppola and Kahn, 1988). Another study addressed the question of which form(s) of sulfur are provided to *R. etli* bacteroids in nodules of common bean. Using a *siroheme synthetase* (*cysG*) mutant of *R. etli* defective in siroheme synthesis, which is required for sulfite reductase activity and in vitro growth on sulfate as sole sulfur source, it was concluded that sulfur compounds other than sulfate can be provided by the host plant to sustain bacteroid nitrogen fixation in common bean nodules (Tate et al., 1997). However, sulfite reductase activity was not measured in the *cysG* mutant bacteroids, and given the fact that *S. meliloti* (http://www.kazusa.or.jp/rhizobase/) and possibly other rhizobia possess more than one *cysG* homolog, it seems premature to conclude that sulfate is not a primary sulfur source for bacteroids in common bean nodules. In any event, given the likely differences in the palette of nutrients that are offered by legumes to their nitrogen-fixing microsymbionts, it may be unwise to extrapolate results from one symbiotic system to another. In the Lotus–*M. loti* system, at least, sulfate appears to be an important source of sulfur for the bacteroids.

Sulfate transporters are encoded by a multigene family in higher plants that consists of five phylogenetically distinct groups (Hawkesford, 2003). For example, *Arabidopsis thaliana* possesses 14 homologous genes encoding confirmed or putative sulfate transporters. Transporters from groups 1 and 2 have been shown to be high- and low-affinity sulfate transporters, respectively (Smith et al., 1995; Takahashi et al., 1997, 2000; Vidmar et al., 2000; Yoshimoto et al., 2002). SST1 belongs to group 3 (Figure 7). Biochemical characteristics together with distinct patterns of gene expression and protein localization indicate that different sulfate transporters fulfill different roles in plants, including high-affinity uptake of soil sulfate into roots, translocation in vascular tissues, and cell-to-cell transfer of sulfate in leaves and seeds (Hawkesford, 2003). Although some plant sulfate transporters are located in the plasma membrane (Kataoka et al., 2004a), at least one has been found elsewhere, on the tonoplast (Kataoka et al., 2004b). Genetic evidence reinforces the notion that plant sulfate transporters have become specialized during evolution, although a certain level of redundancy remains. For instance, physiological analysis of mutant or antisense lines of SULTR1;1 and SULTR1;2 implicate them in sulfate uptake into Arabidopsis roots (Shibagaki et al., 2002; Yoshimoto et al., 2002), although neither alone is crucial for plant sulfur nutrition. On the other hand, a mutant defective in phloem-specific SULTR1;3 revealed that the transporter is necessary, but not indispensable, for efficient long-distance translocation of sulfate in plants (Yoshimoto et al., 2003).

Lotus SST1 exhibits a level of specialization that is unparalleled in other plant sulfate transporters. Loss of activity of this nodule-specific protein in the *sst1-1* and *sst1-2* mutants greatly disrupted SNF and growth in the absence of fertilizer nitrogen (Figures 1 and 3). Thus, somewhat ironically, SST1 is ultimately more important for plant nitrogen nutrition than it is for sulfur nutrition. Nevertheless, the effects of *sst1-1* and *sst1-2* on SNF are presumably mediated through a disruption of sulfur metabolism in the rhizobia, as discussed above. It will be interesting to determine the extent to which bacteroid differentiation is impaired during nodule development in *sst1-1* and *sst1-2*, using DNA microarrays for instance.

Sst1 is not the only sulfate transporter gene that is expressed in Lotus nodules. In fact, several homologs of SST1 can be found in the TIGR database that are expressed in a nodule-specific manner, as judged by their representation in different EST libraries. The other homologs almost certainly perform functions distinct from that of SST1, as none can compensate for the loss of SST1 function in the *sst1* mutants.

Some plant sulfate transporters use a H^+/SO_4^{2-} cotransport mechanism (Lass and Ullricheberius, 1984; Hawkesford et al., 1993; Smith et al., 1995), although it is not clear whether this is true for all sulfate transporters in plants. Interestingly, phylogenetically related mammalian transporters, which group into clades distinct from those of plants, are anion exchangers rather than proton cotransporters (Markovich, 2001). Thus, there is mechanistic diversity within this family of proteins. It seems unlikely that SST1 uses an H^+/SO_4^{2-} cotransport mechanism to transport sulfate into symbiosomes, because the proton motive force is directed out of the symbiosomes toward the cytoplasm (Udvardi and Day, 1997). To date, no member of group 3 of the plant sulfate transporters, including SST1, has been characterized with respect to transport mechanism. In theory, accumulation of anions in symbiosomes is favored by the positive membrane potential on the inside of the SM (Udvardi and Day, 1989; Udvardi et al., 1991). Uptake of sulfate into symbiosomes would also be favored by the removal of sulfate from the symbiosome space by bacteroids, which represent a strong metabolic sink for the anion. It will be exciting to discover whether sulfate transport by SST1 occurs via a mechanism that is independent of proton transport, like its mammalian homologs.

In summary, we have identified the first plant transporter gene, *Sst1*, with a crucial role in SNF in legumes. Although numerous genes involved in nodule development have been identified recently by map-based cloning, *Sst1* is the first gene involved in nodule function to be identified in this way. *Sst1* is expressed in a nodule-specific manner and encodes a functional sulfate transporter. Whereas nodules develop more or less normally on *sst1-1* and *sst1-2* mutant plants, synthesis of nitrogenase is impaired in the rhizobia, which leads to the failure of SNF and early nodule senescence. Based on the data presented here and elsewhere (Wienkoop and Saalbach, 2003), we propose that SST1 transports sulfate from the plant cell cytoplasm to the bacteroids, where the nutrient is crucial for bacterial protein synthesis and other functions.

METHODS

Plant Material and Cultivation

The *Lotus japonicus sst1-1* mutant, originally called *sym13*, was identified in a screen for T-DNA–tagged symbiotic mutants (Schauser et al., 1998), and *sst1-2* (originally called *sym81*) was identified in an independent screen for EMS-mutagenized symbiotic mutants (Kawaguchi et al., 2002).

Plants were grown in a greenhouse in pots containing either quartz sand or clay beads, as described previously (Handberg and Stougaard, 1992; Colebatch et al., 2004), or under sterile conditions on agar plates

containing one-quarter-strength B&D medium (Broughton and Dilworth, 1971) in a growth chamber at 21°C with a 16 h/8 h day/night rhythm.

Transmission Electron Microscopy and Immunogold Labeling

Transmission electron microscopy (TEM) and immunogold labeling were performed as described previously on Lotus nodules (James and Sprent, 1999). Nodules were fixed in 2.5% glutaraldehyde in 0.1 M sodium cacodylate (pH 7.0) overnight at 4°C. The fixed nodules and nodulated roots were either dehydrated in an ethanol series and embedded in LR White acrylic resin (Agar Scientific, Stansted, UK) (James et al., 1996) for light microscopy and TEM immunogold labeling (see below) or postfixed in 1% osmium tetroxide, dehydrated in an ethanol series, and then embedded in Durcupan epoxy resin (Sigma-Aldrich, St. Louis, MO) for conventional TEM. Semithin sections (1 μm) and ultrathin sections (70 nm) were taken from the resin-embedded samples (LR White and Durcupan) using a Reichert Ultracut E ultramicrotome. The semithin sections were collected on glass slides and stained with 1% toluidine blue in borax and viewed and photographed using a BH2 optical microscope (Olympus, Tokyo, Japan). The ultrathin sections for conventional TEM were collected on pioloform-coated copper grids and stained with uranyl acetate (10 min) and lead citrate (5 min) before being viewed with a JEOL 1200 EX transmission electron microscope (JEOL, Tokyo, Japan). Ultrathin sections (70 nm) from LR White–embedded samples were collected as described above, but on nickel grids coated with pioloform. After blocking in a buffer containing 1% Tween 20 and 1% BSA (IGL buffer) (James and Sprent, 1999), the sections were immunogold labeled according to James et al. (1996) with dilutions (in IGL buffer) of antibodies raised against either nitrogenase Fe− (*nifH*) protein (diluted 1:100) or leghemoglobin (diluted 1:100). After washing, 15-nm gold particles conjugated to goat anti-rabbit antibodies (diluted 1:100 in IGL buffer; Amersham, Buckinghamshire, UK) were used to visualize the location of the primary antibody in each case. Samples were viewed with a JEOL 1200 EX transmission electron microscope. The following controls were performed for each immunogold assay: (1) omission of the primary antibody; and (2) substitution of the primary antibody by nonimmune sera diluted appropriately in IGL buffer. Antibodies against leghemoglobin and NifH were obtained from Ton Bisseling (University of Wageningen, The Netherlands) and Paul Ludden (University of California, Berkeley, CA), respectively.

Acetylene Reduction Assay

The acetylene reduction activity of nodulated roots, detached from intact plants, was measured by gas chromatography (Suganuma et al., 1993) after incubation of roots and substrate in a closed 35-mL vial at 25°C for 30 min.

Mapping Population and Positional Cloning

An intraspecific F2 mapping population was created by crossing the Lotus Gifu *sym13* and *sym81* mutants to wild-type Lotus ecotype MG20. F2 homozygous mutant plants were identified on the basis of their fixation minus phenotype. A mapping population consisting of 511 F2 homozygous mutant plants was established. Microsatellite markers developed from TAC clones anchored to the general genetic map of Lotus (Kato et al., 2003) were used to map the *Sst1* locus to a genetic position between markers TM0153 and TM0660. A draft sequence of TAC clone TM0610 was produced, and putative genes were identified by comparison with sequences in the public domain (NCBI).

Gene Expression Analysis

Total RNA was extracted from ~100 mg of plant tissue using an RNeasy kit (Qiagen, Hilden, Germany). One microgram of total RNA was treated with DNaseI, reverse-transcribed, and subjected to quantitative real-time PCR, as described previously (Czechowski et al., 2004). Transcript amounts in different samples were normalized to those of ubiquitin (Colebatch et al., 2004). Gene-specific primers were designed using Primer Express Software (Applied Biosystems, Foster City, CA). The specificity of primer pairs was confirmed by sequencing of PCR amplicons. The following primer sets were used for quantitative real-time PCR: for Sst1, Sst1f (5′-TCTTGGACTGGTCTTCCTTGCT-3′) and Sst1r (5′-TGGTCTCTTGTTCCTCACGTGT-3′); for Ubi, Ubi1f (5′-TTCACCTTGTGCTCCGTCTTC-3′) and Ubi1r (5′-AACAACAGCACACACAGCCAATCC-3′); and for Lb, Lb1f (5′-CTCCAAGCCCATGCTGAAAA-3′) and Lb1r (5′-TGGCATCTGCAAGTGTCACTTC-3′).

PCR Analysis of *sst1* Mutant cDNA

PCR was performed on cDNA from wild-type and *sst1-1* mutant nodules using primers flanking the *sst1-1* mutation site (Ex9-fw [5′-TAGACCTGCAACATGCAAGC-3′] and Ex12-rev [5′-AGAACGATTCCTTCCCAAGC-3′]). The following PCR primers detected *Sst1* cDNA in nodules of wild-type but not *sst1-2* mutant nodules: forward primer 5′-ACCTCATGATGGGAACAAAGAAATGGTAG-3′ and reverse primer 5′-ATGCCCAAGAAGGCCATTCCC-3′. Standard reaction conditions (Sambrook et al., 1989), with an annealing temperature of 56°C, were used for amplification.

Yeast Strains and Functional Complementation

The coding sequence of the *Sst1* cDNA was amplified by PCR using *Pfu* DNA polymerase (Stratagene, La Jolla, CA) and a pair of oligonucleotides containing a 5′ *Pst*I and 3′ *Not*I linker. The amplified fragment was inserted into yeast expression vector p112A1NE (*Pst*I-*Not*I) under the control of the ADH promoter (Riesmeier et al., 1992). The resulting construct was transformed into *Saccharomyces cerevisiae* mutant strain CP154-7A (*Mata*α*, his3, leu2, ura3, ade2, trp1, sul1:LEU2, sul2:URA3*) (Cherest et al., 1997), which is disrupted in the two endogenous yeast sulfate transporters Sul1p and Sul2p, using the lithium acetate method (Gietz et al., 1995). Transformants were selected for Trp prototrophy on yeast nitrogen base medium containing 20 g/L glucose and required amino acids. As controls, empty p112A1NE vector was transformed into the mutant strain, CP154-7A, and a wild-type-like strain, HR1-2B (a gift of Carla Koehler, University of California, Los Angeles, CA). Complementation studies were performed using low-sulfate synthetic minimal medium (Smith et al., 1995) supplied with 20 g/L glucose, required amino acids, and 0.1 to 1 mM $MgSO_4$.

ICP Analysis

Element analysis by ICP-OES was performed as described previously (Becher et al., 2004). Relative total sulfur concentrations were determined by dividing the sulfur concentration in each nodule digest by the magnesium concentration in the same digest. This was done to avoid imprecision in biomass determination of the nodule samples. Plants were grown in a greenhouse for 6 weeks on quartz sand under symbiotic conditions, as described above. Ten to 100 mg of nodule tissue was used for each analysis, with digest volume adjusted according to the mass of material. Three biological replicates were measured.

Sequence Analysis

Sequences were analyzed using the BLAST program and the NCBI database (http://www.ncbi.nlm.nih.gov/BLAST/). Transmembrane protein domains were predicted by transmembrane region detection (http://www.ch.embnet.org/cgi-bin/TMPRED/). Sequence comparisons were performed using Vector NTI software (InforMax, Bethesda, MD).

ACKNOWLEDGMENTS

We thank Vivien Bock, Astrid Schröder, and Diana Sahid for technical support and Björn Usadel for help with phylogenetic analyses. The Max Planck Society, Deutsche Forschungsgemeinschaft, and European Union (HPRN-CT-2000-00086) are thanked for their financial support of this work. L.K. was supported by a grant from Danish Agricultural and Veterinary Research Council.

Received December 9, 2004; accepted March 9, 2005.

REFERENCES

Ampe, F., Kiss, E., Sabourdy, F., and Batut, J. (2003). Transcriptome analysis of *Sinorhizobium meliloti* during symbiosis. Genome Biol. **4,** R15.

Ana, J.M., et al. (2004). *Medicago truncatula* DMI1 required for bacterial and fungal symbioses in legumes. Science **303,** 1364–1367.

Andreev, I., Dubrovo, P., Krylova, V., Andreeva, I.N., Korenkov, V., Sorokin, E.M., and Izmailov, S.F. (1997). Characterization of ATP-hydrolyzing and ATP-driven proton-translocating activities associated with the peribacteroid membrane from root nodules of *Lupinus luteus* L. J. Plant Physiol. **151,** 563–569.

Andreev, I.M., Dubrovo, P.N., Krylova, V.V., and Izmailov, S.F. (1999). Functional identification of ATP-driven Ca^{2+} pump in the peribacteroid membrane of broad bean root nodules. FEBS Lett. **447,** 49–52.

Aravind, L., and Koonin, E.V. (2000). The STAS domain: A link between anion transporters and antisigma-factor antagonists. Curr. Biol. **10,** R53–R55.

Bassarab, S., Mellor, R.B., and Werner, D. (1986). Evidence for 2 types of Mg^{++}-ATPase in the peribacteroid membrane from *Glycine max* root nodules. Endocytobiosis Cell Res. **3,** 189–196.

Becher, M., Talke, I.N., Krall, L., and Kramer, U. (2004). Cross-species microarray transcript profiling reveals high constitutive expression of metal homeostasis genes in shoots of the zinc hyperaccumulator *Arabidopsis halleri*. Plant J. **37,** 251–268.

Becker, A., et al. (2004). Global changes in gene expression in *Sinorhizobium meliloti* 1021 under microoxic and symbiotic conditions. Mol. Plant-Microbe Interact. **17,** 292–303.

Brewin, N.J. (1991). Development of the legume root nodule. Annu. Rev. Cell Biol. **7,** 191–226.

Broughton, W., and Dilworth, M.J. (1971). Control of leghaemoglobin synthesis in snake beans. Biochem. J. **125,** 1075–1080.

Catalano, C.M., Lane, W.S., and Sherrier, D.J. (2004). Biochemical characterization of symbiosome membrane proteins from *Medicago truncatula* root nodules. Electrophoresis **25,** 519–531.

Cherest, H., Davidian, J.C., Thomas, D., Benes, V., Ansorge, W., and Surdin-Kerjan, Y. (1997). Molecular characterization of two high affinity sulfate transporters in *Saccharomyces cerevisiae*. Genetics **145,** 627–635.

Colebatch, G., Desbrosses, G., Ott, T., Krusell, L., Montanari, O., Kloska, S., Kopka, J., and Udvardi, M.K. (2004). Global changes in transcription orchestrate metabolic differentiation during symbiotic nitrogen fixation in *Lotus japonicus*. Plant J. **39,** 487–512.

Colebatch, G., Kloska, S., Trevaskis, B., Freund, S., Altmann, T., and Udvardi, M.K. (2002). Novel aspects of symbiotic nitrogen fixation uncovered by transcript profiling with cDNA arrays. Mol. Plant-Microbe Interact. **15,** 411–420.

Cordoba, E., Shishkova, S., Vance, C.P., and Hernandez, G. (2003). Antisense inhibition of NADH glutamate synthase impairs carbon/nitrogen assimilation in nodules of alfalfa (*Medicago sativa* L.). Plant J. **33,** 1037–1049.

Czechowski, T., Bari, R.P., Stitt, M., Scheible, W.R., and Udvardi, M.K. (2004). Real-time RT-PCR profiling of over 1400 Arabidopsis transcription factors: Unprecedented sensitivity reveals novel root- and shoot-specific genes. Plant J. **38,** 366–379.

Day, D.A., and Copeland, L. (1991). Carbon metabolism and compartmentation in nitrogen-fixing legume nodules. Plant Physiol. Biochem. **29,** 185–201.

Dean, R.M., Rivers, R.L., Zeidel, M.L., and Roberts, D.M. (1999). Purification and functional reconstitution of soybean nodulin 26: An aquaporin with water and glycerol transport properties. Biochemistry **38,** 347–353.

Domigan, N.M., Farnden, K.J.F., Robertson, J.G., and Monk, B.C. (1988). Characterization of the peribacteroid membrane ATPase of lupin root nodules. Arch. Biochem. Biophys. **264,** 564–573.

Dos Santos, P.C., Dean, D.R., Hu, Y.L., and Ribbe, M.W. (2004). Formation and insertion of the nitrogenase iron-molybdenum cofactor. Chem. Rev. **104,** 1159–1173.

El Yahyaoui, F., Kuster, H., Ben Amor, B., Hohnjec, N., Puhler, A., Becker, A., Gouzy, J., Vernie, T., Gough, C., Niebel, A., Godiard, L., and Gamas, P. (2004). Expression profiling in *Medicago truncatula* identifies more than 750 genes differentially expressed during nodulation, including many potential regulators of the symbiotic program. Plant Physiol. **136,** 3159–3176.

Endre, G., Kereszt, A., Kevei, Z., Mihacea, S., Kalo, P., and Kiss, G.B. (2002). A receptor kinase gene regulating symbiotic nodule development. Nature **417,** 962–966.

Fedorova, E., Thomson, R., Whitehead, L.F., Maudoux, O., Udvardi, M.K., and Day, D.A. (1999). Localization of H^{+}-ATPase in soybean root nodules. Planta **209,** 25–32.

Fedorova, M., van de Mortel, J., Matsumoto, P.A., Cho, J., Town, C.D., VandenBosch, K.A., Gantt, J.S., and Vance, C.P. (2002). Genome-wide identification of nodule-specific transcripts in the model legume *Medicago truncatula*. Plant Physiol. **130,** 519–537.

Flemetakis, E., Dimou, M., Cotzur, D., Efrose, R.C., Aivalakis, G., Colebatch, G., Udvardi, M., and Katinakis, P. (2003). A sucrose transporter, LjSUT4, is up-regulated during *Lotus japonicus* nodule development. J. Exp. Bot. **54,** 1789–1791.

Fortin, M.G., Morrison, N.A., and Verma, D.P.S. (1987). Nodulin-26, a peribacteroid membrane nodulin is expressed independently of the development of the peribacteroid compartment. Nucleic Acids Res. **15,** 813–824.

Gaude, N., Tippmann, H., Flemetakis, E., Katinakis, P., Udvardi, M., and Dormann, P. (2004). The galactolipid digalactosyldiacylglycerol accumulates in the peribacteroid membrane of nitrogen-fixing nodules of soybean and Lotus. J. Biol. Chem. **279,** 34624–34630.

Gietz, R.D., Schiestl, R.H., Willems, A.R., and Woods, R.A. (1995). Studies on the transformation of intact yeast cells by the LiAc/SS-DNA/PEG procedure. Yeast **11,** 355–360.

Gordon, A.J., Minchin, F.R., James, C.L., and Komina, O. (1999). Sucrose synthase in legume nodules is essential for nitrogen fixation. Plant Physiol. **120,** 867–878.

Handberg, K., and Stougaard, J. (1992). *Lotus japonicus*, an autogamous, diploid legume species for classical and molecular genetics. Plant J. **2,** 487–496.

Hawkesford, M.J. (2003). Transporter gene families in plants: The sulphate transporter gene family—redundancy or specialization? Physiol. Plant. **117,** 155–163.

Hawkesford, M.J., Davidian, J.C., and Grignon, C. (1993). Sulfate proton cotransport in plasma-membrane vesicles isolated from roots of *Brassica napus* L: Increased transport in membranes isolated from sulfur-starved plants. Planta **190,** 297–304.

James, E.K., and Sprent, J.I. (1999). Development of N-2-fixing

nodules on the wetland legume *Lotus uliginosus* exposed to conditions of flooding. New Phytol. **142,** 219–231.

James, E.K., Iannetta, P.P.M., Nixon, P.J., Whiston, A.J., Peat, L., Crawford, R.M.M., Sprent, J.I., and Brewin, N.J. (1996). Photosystem II and oxygen regulation in *Sesbania rostrata* stem nodules. Plant Cell Environ. **19,** 895–910.

Kaiser, B.N., Moreau, S., Castelli, J., Thomson, R., Lambert, A., Bogliolo, S., Puppo, A., and Day, D.A. (2003). The soybean NRAMP homologue, GmDMT1, is a symbiotic divalent metal transporter capable of ferrous iron transport. Plant J. **35,** 295–304.

Kataoka, T., Hayashi, N., Yamaya, T., and Takahashi, H. (2004a). Root-to-shoot transport of sulfate in Arabidopsis: Evidence for the role of SULTR3;5 as a component of low-affinity sulfate transport system in the root vasculature. Plant Physiol. **136,** 4198–4204.

Kataoka, T., Watanabe-Takahashi, A., Hayashi, N., Ohnishi, M., Mimura, T., Buchner, P., Hawkesford, M.J., Yamaya, T., and Takahashi, H. (2004b). Vacuolar sulfate transporters are essential determinants controlling internal distribution of sulfate in Arabidopsis. Plant Cell **16,** 2693–2704.

Kato, T., Sato, S., Nakamura, Y., Kaneko, T., Asamizu, E., and Tabata, S. (2003). Structural analysis of a *Lotus japonicus* genome. V. Sequence features and mapping of sixty-four TAC clones which cover the 6.4 Mb regions of the genome. DNA Res. **10,** 277–285.

Kawaguchi, M., Imaizumi-Anraku, H., Koiwa, H., Niwa, S., Ikuta, A., Syono, K., and Akao, S. (2002). Root, root hair, and symbiotic mutants of the model legume *Lotus japonicus*. Mol. Plant-Microbe Interact. **15,** 17–26.

Kerppola, T.K., and Kahn, M.L. (1988). Symbiotic phenotypes of auxotrophic mutants of *Rhizobium meliloti* 104a14. J. Gen. Microbiol. **134**, 913–919.

Kouchi, H., et al. (2004). Large-scale analysis of gene expression profiles during early stages of root nodule formation in a model legume, *Lotus japonicus*. DNA Res. **11,** 263–274.

Krusell, L., et al. (2002). Shoot control of root development and nodulation is mediated by a receptor-like kinase. Nature **420,** 422–426.

Kuster, H., et al. (2004). Construction and validation of cDNA-based Mt6k-RIT macro- and microarrays to explore root endosymbioses in the model legume *Medicago truncatula*. J. Biotechnol. **108,** 95–113.

Lass, B., and Ullricheberius, C.I. (1984). Evidence for proton sulfate cotransport and its kinetics in *Lemna gibba* G1. Planta **161,** 53–60.

LeVier, K., Day, D.A., and Guerinot, M.L. (1996). Iron uptake by symbiosomes from soybean root nodules. Plant Physiol. **111,** 893–900.

Levy, J., et al. (2004). A putative Ca^{2+} and calmodulin-dependent protein kinase required for bacterial and fungal symbioses. Science **303,** 1361–1364.

Limpens, E., Franken, C., Smit, P., Willemse, J., Bisseling, T., and Geurts, R. (2003). LysM domain receptor kinases regulating rhizobial Nod factor-induced infection. Science **302,** 630–633.

Lodwig, E.M., Hosie, A.H.F., Bordes, A., Findlay, K., Allaway, D., Karunakaran, R., Downie, J.A., and Poole, P.S. (2003). Amino-acid cycling drives nitrogen fixation in the legume-Rhizobium symbiosis. Nature **422,** 722–726.

Long, S.R. (2001). Genes and signals in the *Rhizobium*-legume symbiosis. Plant Physiol. **125,** 69–72.

Madsen, E.B., Madsen, L.H., Radutoiu, S., Olbryt, M., Rakwalska, M., Szczyglowski, K., Sato, S., Kaneko, T., Tabata, S., Sandal, N., and Stougaard, J. (2003). A receptor kinase gene of the LysM type is involved in legume perception of rhizobial signals. Nature **425,** 637–640.

Markovich, D. (2001). Physiological roles and regulation of mammalian sulfate transporters. Physiol. Rev. **81,** 1499–1533.

Miao, G.H., Hong, Z., and Verma, D.P.S. (1992). Topology and phosphorylation of soybean nodulin-26, an intrinsic protein of the peribacteroid membrane. J. Cell Biol. **118,** 481–490.

Mitra, R.M., Gleason, C.A., Edwards, A., Hadfield, J., Downie, J.A., Oldroyd, G.E.D., and Long, S.R. (2004). A Ca^{2+}/calmodulin-dependent protein kinase required for symbiotic nodule development: Gene identification by transcript-based cloning. Proc. Natl. Acad. Sci. USA **101,** 4701–4705.

Moreau, S., Day, D.A., and Puppo, A. (1998). Ferrous iron is transported across the peribacteroid membrane of soybean nodules. Planta **207,** 83–87.

Moreau, S., Meyer, J.M., and Puppo, A. (1995). Uptake of iron by symbiosomes and bacteroids from soybean nodules. FEBS Lett. **361,** 225–228.

Moreau, S., Thomson, R.M., Kaiser, B.N., Trevaskis, B., Guerinot, M.L., Udvardi, M.K., Puppo, A., and Day, D.A. (2002). GmZIP1 encodes a symbiosis-specific zinc transporter in soybean. J. Biol. Chem. **277,** 4738–4746.

Niemietz, C.M., and Tyerman, S.D. (2000). Channel-mediated permeation of ammonia gas through the peribacteroid membrane of soybean nodules. FEBS Lett. **465,** 110–114.

Nishimura, R., Hayashi, M., Wu, G.J., Kouchi, H., Imaizumi-Anraku, H., Murakami, Y., Kawasaki, S., Akao, S., Ohmori, M., Nagasawa, M., Harada, K., and Kawaguchi, M. (2002a). HAR1 mediates systemic regulation of symbiotic organ development. Nature **420,** 426–429.

Nishimura, R., Ohmori, M., Fujita, H., and Kawaguchi, M. (2002b). A Lotus basic leucine zipper protein with a RING-finger motif negatively regulates the developmental program of nodulation. Proc. Natl. Acad. Sci. USA **99,** 15206–15210.

Ott, T., van Dongen, J., Günther, C., Krusell, L., Desbrosses, G., Vigeolas, H., Bock, V., Czechowski, T., Geigenberger, P., and Udvardi, M.K. (2005). Symbiotic leghemoglobins are crucial for nitrogen fixation in legume root nodules but not for general plant growth and development. Curr. Biol. **15,** 531–535.

Pain, A.N. (1979). Symbiotic properties of antibiotic-resistant and auxotrophic mutants of *Rhizobium leguminosarum*. J. Appl. Bacteriol. **47**, 53–64.

Panter, S., Thomson, R., de Bruxelles, G., Laver, D., Trevaskis, B., and Udvardi, M. (2000). Identification with proteomics of novel proteins associated with the peribacteroid membrane of soybean root nodules. Mol. Plant-Microbe Interact. **13,** 325–333.

Radutoiu, S., Madsen, L.H., Madsen, E.B., Felle, H.H., Umehara, Y., Gronlund, M., Sato, S., Nakamura, Y., Tabata, S., Sandal, N., and Stougaard, J. (2003). Plant recognition of symbiotic bacteria requires two LysM receptor-like kinases. Nature **425,** 585–592.

Riesmeier, J.W., Willmitzer, L., and Frommer, W.B. (1992). Isolation and characterization of a sucrose carrier cDNA from spinach by functional expression in yeast. EMBO J. **11,** 4705–4713.

Rivers, R.L., Dean, R.M., Chandy, G., Hall, J.E., Roberts, D.M., and Zeidel, M.L. (1997). Functional analysis of nodulin 26, an aquaporin in soybean root nodule symbiosomes. J. Biol. Chem. **272,** 16256–16261.

Roberts, D.M., and Tyerman, S.D. (2002). Voltage-dependent cation channels permeable to NH_4^+, K^+, and Ca^{2+} in the symbiosome membrane of the model legume *Lotus japonicus*. Plant Physiol. **128,** 370–378.

Rojas-Ojeda, P., Hernandez, L.E., Brewin, N.J., and Carpena-Ruiz, R. (1998). Comparison of Mg^{2+}-dependent ATP hydrolase activities of pea nodule symbiosomes and of pea root plasmalemma, obtained

by an aqueous polymer two-phase system. J. Chromatogr. B **711,** 139–149.

Roth, E., Jeon, K., and Stacey, G. (1988). Homology in endosymbiotic systems: the term 'symbiosome.' In Molecular Genetics of Plant-Microbe Interactions, R. Palacios and D.P.S. Verma, eds (St. Paul: American Phytopathological Society Press), pp. 220–225.

Roth, L.E., and Stacey, G. (1989). Bacterium release into host-cells of nitrogen-fixing soybean nodules: The symbiosome membrane comes from 3 sources. Eur. J. Cell Biol. **49,** 13–23.

Saalbach, G., Erik, P., and Wienkoop, S. (2002). Characterisation by proteomics of peribacteroid space and peribacteroid membrane preparations from pea (*Pisum sativum*) symbiosomes. Proteomics **2,** 325–337.

Sambrook, J., Fritsch, E.F., and Maniatis, T. (1989). Molecular Cloning: A Laboratory Manual. (Cold Spring Harbor, NY: Cold Spring Harbor Laboratory Press).

Sandal, N., et al. (2002). A genetic linkage map of the model legume *Lotus japonicus* and strategies for fast mapping of new loci. Genetics **161,** 1673–1683.

Schauser, L., Handberg, K., Sandal, N., Stiller, J., Thykjaer, T., Pajuelo, E., Nielsen, A., and Stougaard, J. (1998). Symbiotic mutants deficient in nodule establishment identified after T-DNA transformation of *Lotus japonicus*. Mol. Gen. Genet. **259,** 414–423.

Schauser, L., Roussis, A., Stiller, J., and Stougaard, J. (1999). A plant regulator controlling development of symbiotic root nodules. Nature **402,** 191–195.

Searle, I.R., Men, A.E., Laniya, T.S., Buzas, D.M., Iturbe-Ormaetxe, I., Carroll, B.J., and Gresshoff, P.M. (2003). Long-distance signaling in nodulation directed by a CLAVATA1-like receptor kinase. Science **299,** 109–112.

Shibagaki, N., Rose, A., McDermott, J.P., Fujiwara, T., Hayashi, H., Yoneyama, T., and Davies, J.P. (2002). Selenate-resistant mutants of *Arabidopsis thaliana* identify Sultr1;2, a sulfate transporter required for efficient transport of sulfate into roots. Plant J. **29,** 475–486.

Smil, V. (1999). Nitrogen in crop production: An account of global flows. Global Biogeochem. Cycles **13,** 647–662.

Smith, F.W., Ealing, P.M., Hawkesford, M.J., and Clarkson, D.T. (1995). Plant members of a family of sulfate transporters reveal functional subtypes. Proc. Natl. Acad. Sci. USA **92,** 9373–9377.

Stracke, S., Kistner, C., Yoshida, S., Mulder, L., Sato, S., Kaneko, T., Tabata, S., Sandal, N., Stougaard, J., Szczyglowski, K., and Parniske, M. (2002). A plant receptor-like kinase required for both bacterial and fungal symbiosis. Nature **417,** 959–962.

Suganuma, N., Tamaoki, M., and Takaki, M. (1993). Comparison of the protein composition and enzymatic activities during development between effective and plant-determined ineffective nodules in pea. Plant Cell Physiol. **34,** 781–788.

Takahashi, H., Watanabe-Takahashi, A., Smith, F.W., Blake-Kalff, M., Hawkesford, M.J., and Saito, K. (2000). The roles of three functional sulphate transporters involved in uptake and translocation of sulphate in *Arabidopsis thaliana*. Plant J. **23,** 171–182.

Takahashi, H., Yamazaki, M., Sasakura, N., Watanabe, A., Leustek, T., Engler, J.D., Engler, G., VanMontagu, M., and Saito, K. (1997). Regulation of sulfur assimilation in higher plants: A sulfate transporter induced in sulfate-starved roots plays a central role in *Arabidopsis thaliana*. Proc. Natl. Acad. Sci. USA **94,** 11102–11107.

Tate, R., Riccio, A., Iaccarino, M., and Patriarca, E.J. (1997). A cysG mutant strain of *Rhizobium etli* pleiotropically defective in sulfate and nitrate assimilation. J. Bacteriol. **179,** 7343–7350.

Tyerman, S.D., Whitehead, L.F., and Day, D.A. (1995). A channel-like transporter for NH_4^+ on the symbiotic interface of N-2-fixing plants. Nature **378,** 629–632.

Uchiumi, T., et al. (2004). Expression islands clustered on the symbiosis island of the *Mesorhizobium loti* genome. J. Bacteriol. **186,** 2439–2448.

Udvardi, M.K., and Day, D.A. (1989). Electrogenic ATPase activity on the peribacteroid membrane of soybean (*Glycine max* L) root nodules. Plant Physiol. **90,** 982–987.

Udvardi, M.K., and Day, D.A. (1997). Metabolite transport across symbiotic membranes of legume nodules. Annu. Rev. Plant Physiol. Plant Mol. Biol. **48,** 493–523.

Udvardi, M.K., Lister, D.L., and Day, D.A. (1991). ATPase activity and anion transport across the peribacteroid membrane of isolated soybean symbiosomes. Arch. Microbiol. **156,** 362–366.

Udvardi, M.K., Price, G.D., Gresshoff, P.M., and Day, D.A. (1988). A dicarboxylate transporter on the peribacteroid membrane of soybean nodules. FEBS Lett. **231,** 36–40.

Verma, D.P.S., and Hong, Z.L. (1996). Biogenesis of the peribacteroid membrane in root nodules. Trends Microbiol. **4,** 364–368.

Vidmar, J.J., Tagmount, A., Cathala, N., Touraine, B., and Davidian, J.C.E. (2000). Cloning and characterization of a root specific high-affinity sulfate transporter from *Arabidopsis thaliana*. FEBS Lett. **475,** 65–69.

Weaver, C.D., Shomer, N.H., Louis, C.F., and Roberts, D.M. (1994). Nodulin 26, a nodule-specific symbiosome membrane protein from soybean, is an ion channel. J. Biol. Chem. **269,** 17858–17862.

Wienkoop, S., and Saalbach, G. (2003). Proteome analysis: Novel proteins identified at the peribacteroid membrane from *Lotus japonicus* root nodules. Plant Physiol. **131,** 1080–1090.

Wopereis, J., Pajuelo, E., Dazzo, F.B., Jiang, Q.Y., Gresshoff, P.M., de Bruijn, F.J., Stougaard, J., and Szczyglowski, K. (2000). Short root mutant of *Lotus japonicus* with a dramatically altered symbiotic phenotype. Plant J. **23,** 97–114.

Yoshimoto, N., Inoue, E., Saito, K., Yamaya, T., and Takahashi, H. (2003). Phloem-localizing sulfate transporter, Sultr1;3, mediates re-distribution of sulfur from source to sink organs in Arabidopsis. Plant Physiol. **131,** 1511–1517.

Yoshimoto, N., Takahashi, H., Smith, F.W., Yamaya, T., and Saito, K. (2002). Two distinct high-affinity sulfate transporters with different inducibilities mediate uptake of sulfate in Arabidopsis roots. Plant J. **29,** 465–473.